A Crystalline Metallic Copper Network Application Film Produced by High-Temperature Atmospheric Sintering

Takahiko Kato, *Member, IEEE*, Shuichiro Adachi, Takuya Aoyagi, Takashi Naito, Hiroki Yamamoto, Takeshi Nojiri, and Masato Yoshida

***Abstract*—We show the first production of a copper (Cu) application film (AF) consisting of a novel network of crystalline metallic Cu embedded with copper–phosphorus–oxygen glasses ($Cu_2(PO_4)$ and $Cu_2P_2O_7$) to provide new feedstock materials for crystalline silicon (Si) photovoltaics (PVs). The Cu crystal network was preferentially grown in AF, and thus, a Cu AF with low-electrical resistivity was formed in air at elevated temperatures of $\geq$450 °C by using a copper–phosphorus (Cu–P) alloy paste as a starting material for the sintering. The Cu–P alloy had the role that governed deoxidization of a cuprous oxide, which was formed on heating during the sintering, by virtue of a concurrent oxidation of the Cu phosphide at elevated temperatures. Our results may open the way to the widespread use of atmospherically sintered Cu AFs for mass-production of next-generation crystalline Si PVs.**

***Index Terms*—Atmospheric sintering, copper–phosphorus (Cu–P) alloy paste, crystalline metallic copper application film, crystalline silicon (Si) photovoltaic (PVs) contacts.**

I. Introduction

MATERIAL technology innovations to exchange hazardous, rare, and costly substances for clean and sustainable resources need to be developed for all commoditized mass-produced devices that include the silicon (Si) solar cells of photovoltaic (PV) industries. Silver (Ag) application films (AFs) are widely used in Si solar cells as front-side contacts and backside soldering tabs/pads [1]–[10]. The first attempt to make a crystalline metallic copper (Cu) film rather than an Ag AF used an electroplating technique developed for front-side contacts of a Si solar cell [11]. However, producing Cu AFs by atmospheric sintering, which is currently used for most Ag AFs [1]–[10], would be industrially more attractive because this technique is anticipated to not only exchange rare Ag with more sustainable Cu but to achieve excellent cost performance in both producing the material and processing the crystalline Si PV as well. Sintering is the heat treatment that is applied to AFs to make them electrical conductors; however, Cu oxidizes easily in an atmospheric environment at temperatures of $\geq$200 °C [12]–[15], and the cuprous oxide (Cu_2O) that is formed on heating essentially cannot self-deoxidize in this environment at elevated temperatures because temperatures above its boiling point are required [16], [17]. This has, therefore, restricted the range of temperature to conduct Cu AF studies to $<$200 °C [18], and no Cu AF has yet been produced by an atmospheric sintering process at elevated temperatures $\geq$200 °C.

Here, we report the first production of a crystalline metallic Cu AF in an oxidizing environment during a high-temperature atmospheric sintering process. By using a paste consisting of a copper–phosphorus (Cu–P) alloy with a mixed microstructure of Cu and Cu phosphide (Cu_3P) as a starting material for the sintering, we demonstrated the preferential growth of a crystalline metallic Cu network in air at temperatures $\geq$450 °C and, thus, the formation of a Cu AF with low-electrical resistivity that satisfies the criteria for backside soldering tabs/pads used in crystalline Si PVs. We show the Cu–P alloy has the role that governs deoxidization of Cu_2O, which is formed during the sintering, by virtue of a concurrent oxidation of the Cu_3P at an elevated temperature. The produced Cu AF also has a Cu glass hybrid microstructure in which Cu–P–O glasses ($Cu_2(PO_4)$ and $Cu_2P_2O_7$) are self-assembled and embedded into the opening of the Cu network. Our results may open the way to the widespread use of atmospherically sintered Cu AFs in next-generation crystalline Si PVs.

II. Methodology

Our method to fabricate Cu AFs consists of the atomizing Cu–P alloy particles, forming a Cu–P alloy paste by blending the particles with a solvent and binder, screen-printing the paste onto a substrate, and atmospherically sintering the screen-printed AF. Chemical and physical properties of the atmospherically sintered AFs at various temperatures are finally characterized to clarify the chemical mechanism of the Cu AF creation.

A. Atomization of Copper–Phosphorus Alloy Particles

A high-pressure water atomization furnace with a swirl water jet [19] (Fukuda Metal Foil & Company, Ltd.) was used to

Manuscript received December 2, 2011; revised January 26, 2012; accepted February 2, 2012. Date of publication April 9, 2012; date of current version September 18, 2012.

T. Kato is with the Hitachi Research Laboratory, Hitachi, Ltd., Ibaraki 319-1292, Japan, and also with the Hokkaido University, Sapporo 060-8628, Japan (e-mail: takahiko.kato.ts@hitachi.com).

S. Adachi, T. Nojiri, and M. Yoshida are with the Tsukuba Research Laboratory, Hitachi Chemical Company, Ltd., Tsukuba 300-4247, Japan (e-mail: s-adachi@hitachi-chem.co.jp; t-nojiri@hitachi-chem.co.jp; masa-yoshida@hitachi-chem.co.jp).

T. Aoyagi, T. Naito, and H. Yamamoto are with the Hitachi Research Laboratory, Hitachi, Ltd., Ibaraki 319-1292, Japan (e-mail: takuya.aoyagi.ga@hitachi.com; takashi.naito.gb@hitachi.com; hiroki.yamamoto.gz@hitachi.com).

Color versions of one or more of the figures in this paper are available online at http://ieeexplore.ieee.org.

Digital Object Identifier 10.1109/JPHOTOV.2012.2188018

make Cu–P alloy particles that had a chemical composition of Cu–6.57 mass%P (99.80% purity) (hereafter referred to as Cu–7 mass%P alloy particles), a tap density of 3.85 g/cm^3, a Brunauer–Emmett–Teller specific surface area of 0.3 m^2/g, and a laser 50% diameter of 4.408 μm, as determined by a Nisshin Engineering Inc. turbo-classifier TC-15.

B. Paste Blending

The Cu–P alloy paste was prepared by blending 87.0 mass% Cu–P alloy particles with 12.61 mass% solvent and 0.39 mass% binder, with no glass frit, which is generally used in most Ag AFs [1]–[10] in order to provide good adhesion and electrical contact with the substrate. The solvent was terpineol with an 88.9% purity, 0.932 specific gravity, 1.4834 refractive index, and 0.02 mass% water. The binder was Grade STD200 ethyl cellulose (ethoxized percentage 49%) with a molecular mass of 190.0.

C. Screen-Printing

The Cu–P alloy paste was screen-printed in the form of a 30-μm-thick layer (measured by cross-sectional scanning electron microscopy (SEM) after sintering) onto a 45 mm $\times$ 45 mm area on a Si substrate using a printing press (Microtec Inc., MT-320T) with a printing mask (Sonocom Company, Ltd., KH250-30-60). The substrates were 185-μm-thick P-type single-crystalline Si wafers. The wafer surface was textured using an etching solution of sodium hydroxide and isopropyl alcohol. An n^+-Si layer on the surface of the wafer was formed using phosphorus oxychloride ($POCl_3$). The sheet resistance of the n^+-Si layer was adjusted to 40 Ω/sq. A 90-nm-thick SiN_X layer was deposited onto the front side of the wafer using a PECVD process [20], [21]. The screen-printing was performed on the SiN_X layer-deposited side of the wafer, and the screen-printed AF was then air-dried for 60 s on a conventional hot plate at a temperature of $\leq$150 °C.

D. Atmospheric Sintering

The sintering was performed in an atmospheric environment using a tunnel kiln (Noritake Company Ltd., solar cell heat treatment machine-baking furnace for research and development) that was 507 mm wide internally, 907 mm long, and 523 mm high. The kiln was equipped with a walking beam system consisting of a quartz beam with a stainless pin that was used to transport the Si-wafer through the centre of the kiln. Sintering was performed in an atmospheric environment over the temperature range of 300–500 °C, while the temperature was increased in a stepwise fashion at 50 °C intervals. The temperature was controlled in three sequential heating zones, the first and second of which were used as preheating zones and the third of which was set to the desired sintering temperature. The first and second heating zones were held at 300 °C unless the sintering temperature was 500 °C, in which case, the first and second preheating temperatures were 300 and 305 °C, respectively. Each zone was heated using ten near-infrared heaters, each 15 kW in capacity, placed above and below the beam position of the Si-wafer transportation system. The screen-printed film samples were continuously transported through the three zones, spending 10 s in each zone. The airflow inside the tunnel kiln was controlled using air intakes and exhaust ejectors mounted in each temperature zone. For the first and last zones, the flow through the air intakes was 50 l/min, and the flow through the exhausts was 80 l/min. The flow was zero for the intake and exhaust in the second zone. An 80-l/min air curtain was situated in a duct located between the sample entrance and the first preheating zone.

E. Characterization of Atmospherically Sintered Application Films

The atmospherically sintered AFs were characterized using field-emission SEMs (Hitachi S-4800 and SU-70) observation, energy dispersive X-ray spectroscopy (EDX) (Horiba EX-350) analysis, electron backscattering pattern (EBSP) (TSL MSC-2200) measurements using a 20-kV acceleration voltage and a 0.13-μm step size, X-ray diffraction (XRD) (Rigaku RINT2500HL) using Cu Kα radiation, and electrical conductivity measurements using an ac four-probe method (Mitsubishi Chemical Loresta-EP MCP-360 and Hiresta-UP MCP-HT450). The XRD measurements were performed using the focusing beam method ($2\theta-\theta$ rotation mechanism) with an X-ray output of 50 kV–250 mA, which allowed the whole thickness of the AFs to be probed. Continuous scans were performed over the 2θ range of 5–100° with a scanning rate of 0.5°/min. A 5° soller slit, 0.5° divergence slit, 0.5° scattering slit, and 0.15-mm receiving slit were incorporated into the XRD system. Data were sampled at steps of 0.01°. The integrated peak intensity associated with a given crystalline phase was analyzed as follows: First, peaks were identified and indexed on the basis of the crystal structures listed in the International Centre for Diffraction Data database; second, the data for the instrumental peak width were corrected using a standard sample (NIST-Si); third, the integrated intensities and widths of peaks were estimated by profile fitting; and fourth, the integrated intensity ratio for each phase was calculated by summing the integrated intensities of peaks associated with that phase and dividing them by the total sum of peak intensities for all phases.

Thermogravimetry-differential thermal analysis (TG-DTA) (Shimazu DTG60H) was also performed in an atmospheric environment with an airflow of 50 ml/min and a heating rate of 0.167 °C/s (10 °C/min) in order to understand oxidation behavior of Cu_3P phase. Samples of 30 mg in mass were loaded into an alumina cell as follows: as-atomized Cu-7 mass%P alloy particles with an average diameter of $\sim$1 μm and pure Cu_3P particles with diameters of $<$300 μm and a purity of $>$99.0% (Kojundo Chemical Laboratory Company, Ltd., Cu_3P powder sieved through a 300 μm mesh) were used for the TG-DTA.

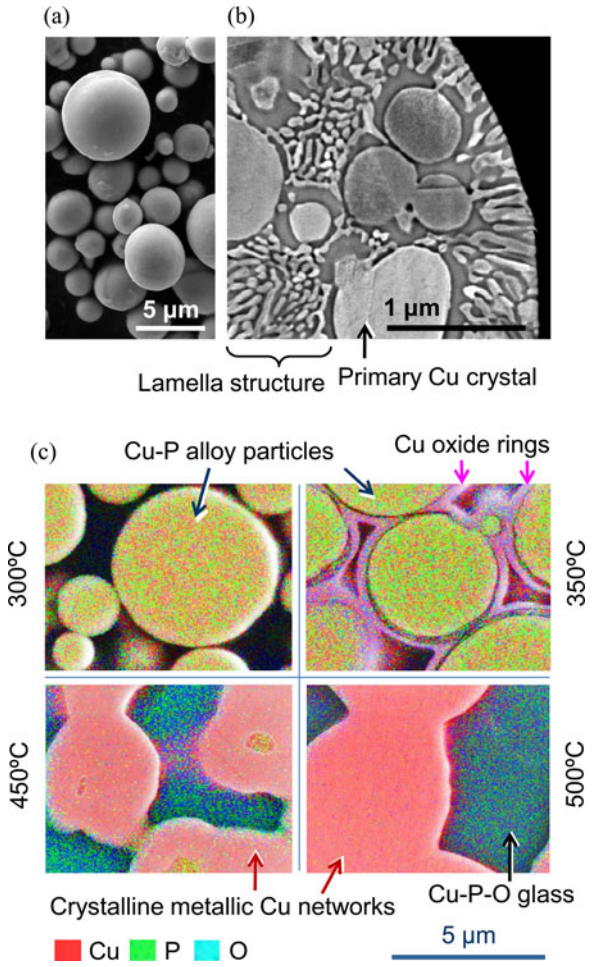

Fig. 1. Atmospheric sintering forms a crystalline metallic Cu network. (a) SEM secondary electron image of as-atomized starting material (Cu–P alloy particles) showing spherical shape. (b) Cross-sectional SEM backscattered electron image of an individual particle showing the pro-eutectic microstructure. Primary Cu crystals are evident, between which the eutectic consisting of Cu and Cu_3P is visible as a lamellar structure. (c) Cross-sectional SEM secondary electron images showing the shapes of the alloy particles, with the elemental distribution (determined by EDX) mapped onto the images, in screen-printed AF samples atmospherically sintered at temperatures from 300 to 500 °C.

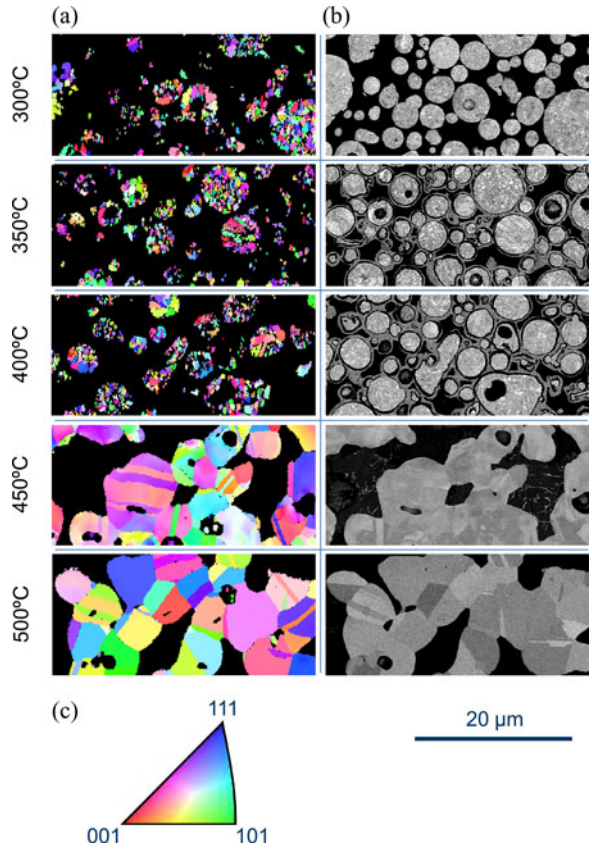

Fig. 2. Crystalline metallic Cu network generated by oxidizing small Cu crystals in Cu–P alloy particles followed by deoxidizing Cu_2O. (a) IPF maps (derived from EBSP measurements) showing the evolution of crystalline Cu distribution in cross sections of screen-printed AFs atmospherically sintered at the indicated temperatures. (b) SEM backscattered electron images corresponding to the IPF maps in (a). (c) Color code for Cu crystal orientations in the IPF maps shown in (a).

III. Results

A. Producing Copper Application Films by Atmospheric Sintering

Fig. 1(a) shows spherical Cu–P alloy particles produced using a high-pressure water atomization furnace with a swirl water jet that had a chemical composition of Cu–7 mass%P. Fig. 1(b) shows a cross-sectional view of a typical as-atomized Cu–7 mass%P particle. A proeutectic microstructure is evident, which is consistent with the Cu–P binary alloy phase diagram [22].

The screen-printed and dried Cu–P alloy paste AF were sintered in an atmospheric environment by increasing the temperature from 300 to 500 °C at intervals of 50 °C, with a holding time of 10 s at each temperature. The sintering drastically changed both the shape of the Cu–P alloy particles in the AF and the distribution of the elements within the particles. Fig. 1(c) shows micrographs depicting the distribution of Cu (red), P (green), and oxygen (O; blue) determined by EDX analysis, mapped onto an SEM secondary electron image with the same cross-sectional field. The yellowish particles were not oxidized at 300 °C, whereas Cu_2O rings appeared around the particles, visible as light pink fringes, at 350 °C. At temperatures of ≥450 °C, both the microstructure and the elemental distribution drastically changed: A crystalline metallic Cu network was formed, and a Cu–P–O glass was self-assembled in the openings of the network. Evidence is given later of the formation of the crystalline metallic Cu network by EBSP measurement. The Cu network appears pink in the SEM images because it contains a small amount of P (between 0.31 and 0.44 mass% as determined by EDX analysis) in the form of a dilute solid solution.

B. Indicating Crystalline Metallic Copper Network

Fig. 2(a) shows inverse pole figure (IPF) maps (derived from EBSP measurements) of crystalline metallic Cu with the face-centered cubic lattice formed during the atmospheric sintering; Fig. 2(b) shows the corresponding SEM micrographs. At temperatures ≤400 °C, metallic Cu was found only in the form of small crystals within the Cu–P alloy particles; at temperatures ≥450 °C, a crystalline metallic Cu network with larger,

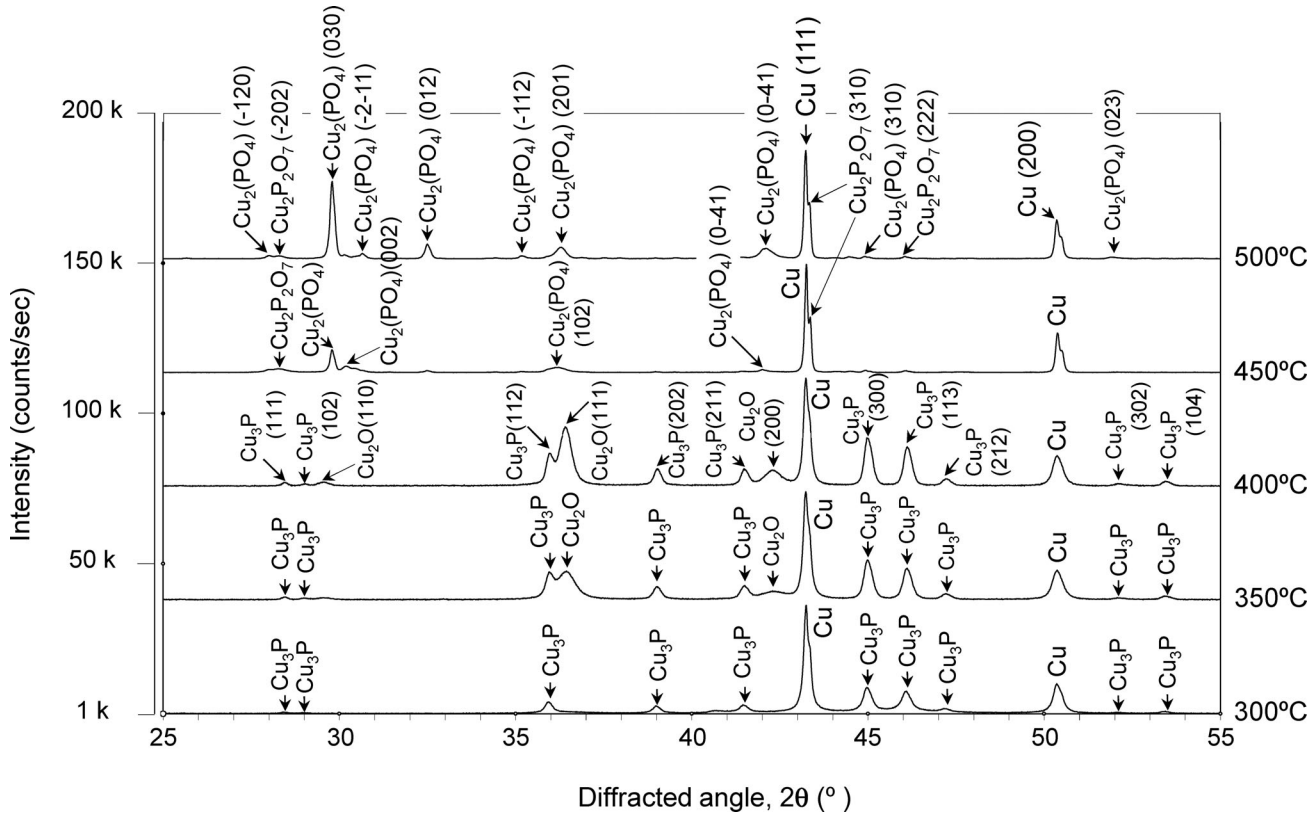

Fig. 3. XRD patterns for the screen-printed and atmospherically sintered AFs characterized in Figs. 1 and 2.

unoriented grains was formed. The grains were completely interconnected to form a network, and some of the grains exhibited stripes, which were probably twin structures. We can thus conclude that the key reactions involved in the formation of the metallic Cu network—that is, the annihilation of fine-grained Cu formed by oxidation of the starting material and the subsequent generation of large-grained crystalline metallic Cu network by deoxidizing Cu_2O—must occur at temperatures between 400 and 450 °C.

C. Chemical Mechanism of Copper Application Film Formation

We used XRD to evaluate the fractions of phases present in AFs formed at different sintering temperatures, and the results are shown in Fig. 3 (XRD patterns) and Fig. 4 (integrated XRD peak intensity ratios) along with the corresponding electrical resistivities. The XRD patterns of all the examined AFs showed crystalline peaks (see Fig. 3); no halo patterns arising from amorphous substances were evident. No Cu oxide species were observed at 300 °C, which is consistent with the microstructure [see Fig. 1(c)]. When the sintering temperature was raised to 350 °C and then to 400 °C, Cu_2O appeared and its fraction increased, whereas that of crystalline metallic Cu decreased and that of Cu_3P remained almost unchanged [see Fig. 4(a)]. No P–O compounds were detected. Evidently, Cu_2O is deoxidized at 450 °C because a rapid increase in the fraction of crystalline Cu occurred at that temperature (reaching an integrated intensity ratio of 66.9%), along with a corresponding decrease in the ratio of Cu_2O to 12.0%. This reaction takes place in conjunction with the oxidation of Cu_3P; the Cu_3P disappeared, and the new compounds $Cu_2(PO_4)$ and $Cu_2P_2O_7$ appeared at 450 °C. We can thus conclude that the Cu–P alloy governs the deoxidization of Cu_2O by virtue of the concurrent oxidation of Cu_3P, and that Cu_3P acts as a suitable reducing agent for Cu_2O in the atmospherically sintered AF. Our XRD results imply that the following two reactions take place simultaneously and that reaction (2) largely contributes to the rapid increase in metallic Cu at 450 °C

$$2\mathrm{Cu} + \frac{1}{2}\,\mathrm{O_2} \rightarrow \mathrm{Cu_2O} \tag{1}$$

$$\mathrm{Cu_2O} + 3\mathrm{Cu_3P} + 5\mathrm{O_2} \rightarrow 7\mathrm{Cu} + \mathrm{Cu_2(PO_4)} + \mathrm{Cu_2P_2O_7}. \tag{2}$$

Reaction (3), shown below, is also likely to be accelerated at higher temperatures because, as shown in Fig. 4(a), the fraction of $Cu_2(PO_4)$ increased and the fractions of both Cu and $Cu_2P_2O_7$ decreased at 500 °C

$$2\mathrm{Cu} + \mathrm{Cu_2P_2O_7} + \frac{1}{2}\,\mathrm{O_2} \rightarrow 2\mathrm{Cu_2(PO_4)}. \tag{3}$$

Furthermore, the XRD results indicate that the Cu–P–O glass, which is self-assembled and embedded into the openings of the Cu network [see Fig. 1(c)], consists of two crystalline phases: $Cu_2(PO_4)$ and $Cu_2P_2O_7$. As shown in Fig. 4(b), the electrical resistivity of the AF was dramatically reduced at sintering temperatures of 450 °C and 500 °C ($2.40 \pm 0.58 \times 10^{-5}$ Ω·cm and

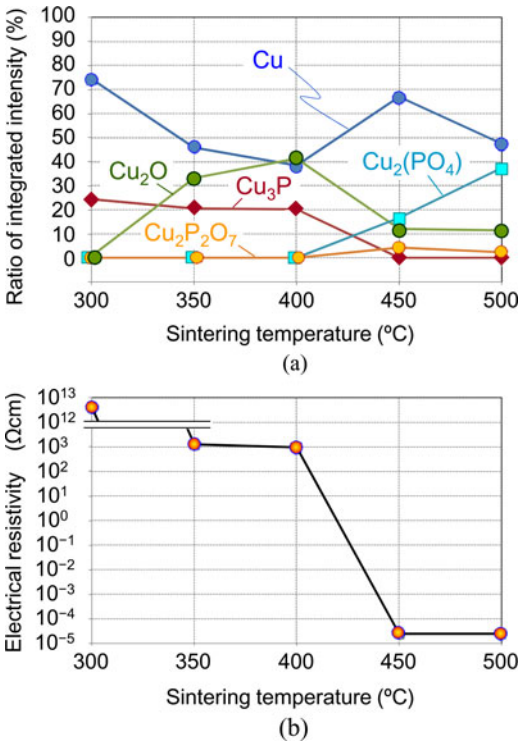

Fig. 4. Deoxidizing Cu_2O leads to growth of crystalline Cu and dramatic reduction in electrical resistivity. (a) Integrated XRD peak intensity ratios for all the crystalline phases in the screen-printed AFs characterized in Figs. 1 and 2. (b) Corresponding electrical resistivity for the AFs in (a).

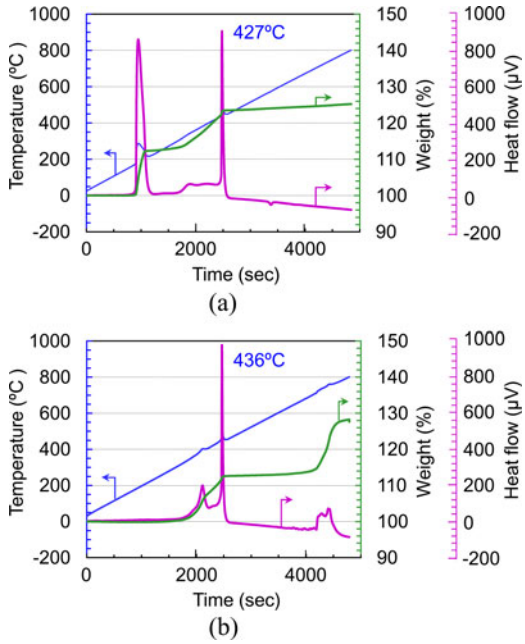

Fig. 5. Oxidizing Cu_3P probed by TG-DTA. (a) Heat flow (purple), weight (green), and temperature (blue) plots for as-atomized Cu-7 mass%P alloy particles with an average diameter of ∼1 μm showing exothermic heat flow peak at ∼430 °C. (b) Corresponding heat flow, weight, and temperature plots for pure Cu_3P particles with diameters of <300 μm.

$2.46 \pm 0.78 \times 10^{-5}$ Ω·cm, respectively), at which a network of crystalline metallic Cu (containing between 0.31 and 0.44 mass% P) was formed. The AFs with such electrical resistivity satisfied the criteria for backside soldering tabs/pads used in crystalline Si PVs.

IV. Discussion

The results shown in Figs. 1–4 suggest that Cu_2O should deoxidize due to Cu_3P oxidizing [expressed by reaction (2)] at temperatures between 400 and 450 °C. We confirmed this by performing TG-DTA measurements on the as-atomized Cu-7 mass%P alloy particles and on pure Cu_3P particles (see Fig. 5), in the absence of a solvent, binder, or glass frit. The heat-flow plots for both the Cu–7 mass%P alloy and the Cu_3P particles sharply peaked at ∼430 °C [see Fig. 5(a) and (b)].

The sharp exothermic peak observed at ∼200 °C for the Cu–7 mass%P alloy particles is thought to be caused by Cu oxidizing within the particles. That Cu rapidly oxidizes at temperatures between 200 and 250 °C is an established phenomenon [14], [15], although the AF sample that contained the solvent (terpineol) and binder (ethyl cellulose) and was sintered at 300 °C showed no evidence of Cu oxidizing inside the Cu–7 mass%P alloy particles [see Figs. 1(c) and 4(a)]. The terpineol is vaporized before sintering so that the binder seems to prevent Cu oxidizing at temperatures up to 300 °C, at which point, it starts to burn (as confirmed by TG-DTA). Further, efforts should, therefore, be made to optimize the properties of the atmospherically sintered Cu AFs by exploring the potential of alternative solvent, binder, and glass-frit materials.

More advanced studies on the Cu AFs developed in this paper will also provide various solutions for practical requirements of backside soldering tabs/pads used in various types of Si PVs, for example, forming a self-assembled conductive barrier between the Cu AF and Si wafer, joining tab leads to the Cu AFs, and improving the Cu AFs so that they can be formed through a sintering process at higher temperatures similar to those of aluminium paste or Ag paste sintering processes used for present crystalline Si PVs.

V. Conclusion

We reported the first production of a Cu AF consisting of a novel network of crystalline metallic Cu embedded with self-assembled Cu–P–O glasses ($Cu_2(PO_4)$ and $Cu_2P_2O_7$) that are grown in the sintering process using air at temperatures of ≥450 °C. For the Cu AF production, we developed a starting paste material composed of Cu–P alloy particles with a mixed microstructure of Cu and Cu_3P phases. The Cu AF has electrical resistivity that satisfies the criteria for backside soldering tabs/pads used in crystalline Si PVs. Our study clarifies in detail the production method used for the Cu AFs and the chemical mechanism of their creation, as well as characterizing in detail the chemical and physical properties of the films. Our results may open the way to the widespread use of atmospherically sintered Cu AFs in next-generation crystalline Si PVs.

ACKNOWLEDGMENT

The authors acknowledge the valuable scientific discussions with S. Watanabe, N. Sakaguchi, S. Miura (Hokkaido University), M. Iwamuro, S. Takeda, K. Okaniwa, M. Kim, M. Katayose (Hitachi Chemical Company, Ltd.), Y. Sawai, and N. Tanaka (Hitachi, Ltd.).

REFERENCES

[1] E. L. Ralph, "Recent advancements in low cost solar cell processing," in *Proc. 11th IEEE Photovoltaic Spec. Conf.*, New York, 1975, pp. 315–316.
[2] A. D. Haigh, "Fired through printed contacts on antireflection coated silicon terrestrial solar cells," in *Proc. 12th IEEE Photovoltaic Spec. Conf.*, Baton Rouge, LA, 1976, pp. 360–361.
[3] H. C. Lin, D. P. Spittlehouse, and Y. W. Hsueh, "Contact resistance of silver ink on solar cell," in *Proc. 13th IEEE Photovoltaic Spec. Conf.*, Washington, DC, 1978, pp. 593–596.
[4] C. Ballif, D. M. Huljić, A. Hessler-Wyser, and G. Willeke, "Nature of the Ag-Si interface in screen-printed contacts: A detailed transmission electron microscopy study of cross-sectional structures," in *Proc. 29th IEEE Photovoltaic Spec. Conf.*, New Orleans, LA, 2002, pp. 360–363.
[5] G. Schubert, B. Fischer, and P. Fath, "Formation and nature of Ag thick film front contacts on crystalline silicon solar cells," in *Proc. Photovoltaic Eur. Conf.*, Rome, Italy, 2002, pp. 343–346.
[6] C. Ballif, D. M. Huljić, G. Willeke, and A. Hessler-Wyser, "Silver thick-film contacts on highly doped n-type silicon emitters: structural and electronic properties of the interface," *Appl. Phys. Lett.*, vol. 82, pp. 1878–1880, 2003.
[7] G. Schubert, F. Huster, and P. Fath, "Current transport mechanism in printed Ag thick film contacts to an n-type emitter of a crystalline silicon solar cell," in *Proc.19th Eur. Photovoltaic Sol. Energy Conf.*, Paris, France, 2004, p. 813.
[8] M. M. Hilali, A. Rohatgi, and B. To, "A review and understanding of screen-printed contacts and selective-emitter formation," in *Proc. 14th Workshop Crystalline Silicon Sol. Cells Modules*, 2004, pp. 1–8.
[9] G. Schubert, J. Horzel, R. Kopecek, F. Huster, and P. Fath, "Silver thick film contact formation on lowly doped phosphorous emitters," in *Proc. 20th Eur. Photovoltaic Sol. Energy Conf.*, Barcelona, Spain, 2005, pp. 2–5.
[10] D.-H. Neuhaus and A. Münzer, "Industrial silicon wafer solar cells," *Adv. OptoElectron.*, vol. 2007, Art. ID 24521, pp. 1–15, 2007.
[11] C. E. Dube and R. C. Gonsiorawski, "Improved contact metallization for high efficiency EFG polycrystalline silicon solar cells," in *Proc. 21th IEEE Photovoltaic Spec. Conf.*, Kissimmee, FL, 1990, vol. 1, pp. 624–628.
[12] H. A. Miley, "Copper oxide films," *J. Amer. Chem. Soc.*, vol. 59, pp. 2626–2629, 1937.
[13] W. E. Campbell and U. B. Thomas, "The oxidation of metals," *Trans. Electrochem. Soc.*, vol. 91, pp. 623–640, 1947.
[14] S. Shirai, "On the oxidation of the thin single crystal film of copper," *J. Phys. Soc. Jpn.*, vol. 2, pp. 81–83, 1947.
[15] H. Wieder and A. W. Czanderna, "The oxidation of copper films to $CuO_{0.67}$," *J. Phys. Chem.*, vol. 66, pp. 816–821, 1962.
[16] H. J. T. Ellingham, "Reducibility of oxides and sulphides in metallurgical processes," *J. Soc. Chem. Ind.*, vol. 63, pp. 125–133, 1944.
[17] F. D. Richardson and J. H. E. Jeffes, "The thermodynamics of substances of interest in iron and steel making from 0 °C to 2400 °C: I-Oxides," *J. Iron Steel Inst.*, vol. 160, pp. 261–270, 1948.
[18] M. Yoshida, H. Tokuhisa, U. Itoh, I. Sumita, S. Sekine, and T. Kamata, "Glass-fritless Cu alloy pastes for silicon solar cells requiring low temperature sintering," in *Proc. 26th Eur. Photovoltaic Sol. Energy Conf. Exhib.*, Hamburg, Germany, 2011, pp. 858–860.
[19] M. Kikukawa, S. Matsunaga, T. Inaba, O. Iwatsu, and T. Takeda, "Development of spherical fine powders by high-pressure water atomization using swirl water jet," *J. Jpn. Soc. Powder Powder Metall.*, vol. 47, pp. 453–457, 2000.
[20] A. G. Aberle, "Overview on SiN surface passivation of crystalline silicon solar cells," *Sol. Energy Mater. Sol. Cells*, vol. 65, pp. 239–248, 2001.
[21] F. Duerinckx and J. Szlufcik, "Defect passivation of industrial multicrystalline solar cells based on PECVD silicon nitride," *Sol. Energy Mater. Sol. Cells*, vol. 72, pp. 231–246, 2002.
[22] S. An Mey and P. J. Spencer, "A thermodynamic evaluation of the copper-phosphorus system," *Calphad*, vol. 14, pp. 265–274, 1990.

Takahiko Kato (M'08) received the B.E., M.E., and Ph.D. degrees in materials science from Hokkaido University, Sapporo, Japan.

Since 1982, he has been with Hitachi, Ltd., Ibaraki, Japan. As a Group Leader of materials technology with various Hitachi sections, he has researched materials related to boiling-water reactors, fusion reactors, and superconductors. As a Chief Researcher with Hitachi Research Laboratory, Hitachi, Ltd., he has expanded his research areas to electrical-device materials and sustainable energy device materials. He is also a Guest Professor with Hokkaido University in the field of materials science.

Dr. Kato is a member of the IEEE Components, Packaging, and Manufacturing Technology (CPMT) and Electron Devices Societies, the Japan Institute of Electronic Packaging, and the Japan Institute of Metals. In 2011, he was presented with the 2010 IEEE CPMT Transactions Best Paper Award for "Correlation between whisker initiation and compressive stress in electrodeposited tin-copper coating on copper leadframes," in the IEEE TRANSACTIONS ON ELECTRONICS PACKAGING MANUFACTURING, vol. 33, no. 3, July 2010.

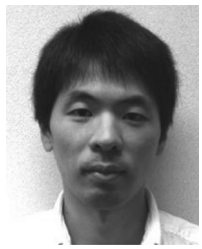

Shuichiro Adachi received the B.E. and M.E. degrees in material science from the Tokyo University of Science, Chiba, Japan.

Since 2005, he has been with the Hitachi Chemical Company, Ltd., Ibaraki, Japan. He developed the manufacturing process of alumina ceramics by the direct casting method. In 2009, he transferred to the laboratory for energy-related materials of Hitachi Chemical Company, Ltd., where he changed his research area to Cu-based materials applied to photovoltaic electrodes.

Mr. Adachi is a member of the Ceramic Society of Japan.

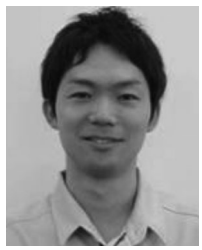

Takuya Aoyagi received the B.S. and M.S. degrees in applied chemistry from Tohoku University, Sendai, Japan.

In 2008, he joined Hitachi Research Laboratory, Hitachi, Ltd., Ibaraki, Japan, where he has been engaged in the research and development of glassy materials technology and manufacturing processes for glass metal hybrid electrodes for sustainable energy devices.

Mr. Aoyagi is a member of the Japan Society of Applied Physics and the Ceramic Society of Japan.

Takashi Naito received the B.E. and M.E. degrees in applied chemistry from Keio University, Yokohama, Japan.

In 1983, he joined Hitachi Research Laboratory, Hitachi, Ltd., Ibaraki, Japan, where he has been involved in the research and development of glassy materials technology and manufacturing processes for glass metal hybrid electrodes for sustainable energy devices.

Mr. Naito is a member of the Ceramic Society of Japan.

Hiroki Yamamoto received the B.Sc., M.Sc., and D.Sc. degrees in inorganic material science from the Tokyo Institute of Technology, Tokyo, Japan.

Since 1993, he has been with the Hitachi Research Laboratory, Hitachi, Ltd., Ibaraki, Japan, and has developed a low melting glass for electronic devices and a thin film technique for optical recording media.

Dr. Yamamoto is a committee member of the Japan Society of Applied Physics and the Ceramic Society of Japan.

Takeshi Nojiri received the B.S. and M.S. degrees in applied chemistry from Tokyo Metropolitan University, Tokyo, Japan.

In 1990, he joined the Ibaraki Research Laboratory of Hitachi Chemical Company, Ltd., Ibaraki, Japan, where he was involved in the research and development of photosensitive film for printed circuit boards and liquid crystal displays. In 2009, he transferred to Tsukuba Research Laboratory, Ibaraki, Japan, where he has been involved in materials and process development for sustainable energy devices.

Mr. Nojiri is a member of the Ceramic Society of Japan.

Masato Yoshida received the B.E., M.E., and Ph.D. degrees in applied chemistry from the Tokyo Institute of Technology, Tokyo, Japan.

In 1987, he joined the Tsukuba Research Laboratory of Hitachi Chemical Company, Ltd., Ibaraki, Japan. He developed the chemical mechanical polishing slurry for fabricating semiconductors.

Dr. Yoshida is a member of the Japan Institute of Metals and the Japan Institute of Energy.